

Supplemental Materials

Molecular Biology of the Cell

Koestler et al.

Online Supplemental Material

Supplemental Figure legends

Figure S1: WCA/Rac-injection specifically blocks Arp2/3-, but not Spir-mediated actin polymerization.

(A) Fluorescence images of an NIH3T3 cell expressing EGFP-MBD-WWCA (left), targeting to and driving Arp2/3-dependent actin assembly at microtubules (highlighted as yellow structures before injection on the right; Oelkers *et al.*, 2011), and mCherry-actin (middle) before (top) and 15 minutes after microinjection of WCA/Rac (bottom). Right panels show merges of EGFP and mCherry channels. Note loss of actin accumulation on microtubules upon microinjection (middle), also highlighted as green tubules lacking actin on the right. Bar, 5 μm .

(B) Fluorescence images of an NIH3T3 cell expressing EGFP-MBD-SpirNT (left), driving robust actin assembly on the surface of microtubules (Oelkers *et al.*, 2011), and mCherry-actin (middle) before and 15 minutes after microinjection of WCA/Rac1. Right panels show merges of EGFP and mCherry channels, and confirm absence of interference with Spir-driven actin assembly through Arp2/3 complex sequestration. Bar, 5 μm .

Figure S2: Expression of tropomyosin isoforms.

Western blots of extracts prepared from NIH3T3 cells transfected with EGFP/EYFP-tagged Tm constructs as indicated, and incubated with primary Tm or GFP antibodies.

Figure S3: Arp2/3 complex inhibition does not affect localization of high (Tm3) or low (Tm5NM1) molecular weight tropomyosins.

Fluorescence (green in merges) and phase contrast (red in merges) images of cells transfected with constitutively active Rac1 and EGPF-tagged Tm3 or Tm5NM1 before and after injection of WCA/Rac1 as indicated. Time is in minutes and seconds. Cell peripheries are devoid of Tm isoforms before and after Arp2/3 complex inhibition.

Figure S4: Loss of lamellipodial cofilin is not accompanied by Tm2 accumulation:

Dual-color fluorescence and phase contrast images of NIH3T3 cell co-expressing mCherry-cofilin and EGFP-Tm2 before and at different time points after injection with WCA/Rac1, as indicated. Right column shows merges of EGFP-Tm2 (green) and phase contrast (red). Time, minutes and seconds.

Figure S5:

(A) WAVE2 turnover in the lamellipodium is independent of Arp2/3-complex.

FRAP experiments of EGFP-WAVE2 at the cell periphery in NIH3T3 cells expressing constitutively active Rac1, and injected with Rac1 (top) or WCA/Rac1 (bottom). White rectangles indicate bleach regions. Time is given in seconds, bars represent 5 μm . Right: Graphs displaying mean curves of individually fitted recovery of fluorescence after photobleaching. Red lines indicate half times of recovery ($t_{1/2}$). Error bars are SEM, n corresponds to cell number analyzed.

(B) CA does not interfere with spontaneous, Arp2/3-independent actin polymerization.

A total of 2 μM G-actin (10% pyrene-labeled) was polymerized in 1 x KMEI buffer in presence of CA at concentrations as indicated. Note that not even a 10 times molar excess of CA over actin affected actin polymerization significantly.

(C) Cofilin and capping protein (CP) do not co-precipitate with Arp2/3 complex.

Pull-downs with GST-WCA of Arp2/3-complex in the presence or absence of cofilin or capping protein (CP), as indicated. GST-WCA-coupled beads were incubated with 5 μ M CP or 5 μ M cofilin-1 as additional controls. Purified proteins are shown on the left (input). Note that in spite of significant pull-down of Arp2/3 complex, no interaction was detected for either CP or cofilin-1. In addition, neither protein showed direct interaction with WCA alone. Coomassie-blue staining of 15% SDS-PAGE gel.

Figure S6: Reversible inhibition of Arp2/3 accumulation by transient CK666 treatment.

Fluorescence and phase contrast video frames of B16-F1 cells expressing EGFP-p16B (upper panel) or EGFP-actin (lower panel) before and after CK666 treatment followed by inhibitor washout. Time is given in minutes and seconds before and after inhibitor addition or washout, as indicated. Inset diagrams depict line scans of fluorescence signal intensities of respective proteins. Measured regions are boxed in images. Black and red lines show intensities before and after CK666 treatments, respectively. Note marked and reversible reduction of Arp2/3 complex accumulation during CK666 treatment. CK666 also reduces actin filament intensity at the cell periphery, as expected, but less prominently than that of Arp2/3 complex. Bars, 3 μ m.

Figure S7: Transient Arp2/3 inhibition by CK666 reversibly reduces cofilin and capping protein accumulation.

Selected frames of fluorescence and phase contrast movies of B16-F1 cells expressing EGFP-cofilin (upper panel) or EGFP-tagged capping protein β 2 (CP, lower panel) and transiently treated with CK666 as indicated. Time is in minutes and seconds before and after inhibitor addition or washout. Inset diagrams show line scans of fluorescence signal intensities of respective proteins measured from respective regions boxed in images. Black and red lines show intensities before and after CK666 treatments, respectively. Note significant, reversible

reduction of cofilin and CP localization at the cell periphery during Arp2/3 inhibition. Bars, 3 μm .

Figure S8: Ultrastructural rearrangements following Rac1- or WCA/Rac1-injections in fish keratocytes.

Electron tomograms of leading edges of Rac1- (top) or WCA/Rac1- (bottom) injected, negatively-stained fish keratocytes. Bars represent 200 nm.

Movie legends

Movie S1: Phase contrast movies of NIH3T3 cells transfected with constitutively active Rac1 and recorded before and after microinjection with WCA/Rac1 (right) or Rac1 alone (left) as control. Time is in minutes and seconds, bar: 10 μm .

Movie S2: Fluorescence time lapse microscopy of NIH3T3 cells co-transfected with constitutively active Rac1 and EGFP-Lifeact (labels actin filaments). The cell on the left is shown before and after microinjection with WCA/Rac1, as indicated. Time is in minutes and seconds.

Movie S3: FRAP of EGFP-actin at edges of Rac1- and WCA/Rac1-injected NIH3T3 cells (left and right panels, respectively) co-expressing constitutively active Rac1. Time is in seconds, bar: 3 μm .

Movie S4: Electron tomograms through edges of Rac1- and WCA/Rac1-injected NIH3T3 cells transfected with constitutively active Rac1. Bar: 100 nm.

Movie S5: Fluorescence (left) and phase contrast (right) time-lapse microscopy of NIH3T3 cell co-transfected with constitutively active Rac1 and EGFP-tagged myosin light chain before and after microinjection WCA/Rac1, as indicated. White arrowheads mark appearance of myosin spots distal to the lamellipodium-lamella boundary shortly after WCA/Rac1 injection. Time is in minutes and seconds, bar: 5 μm .

Movie S6: Fluorescence movies of EGFP-tagged proteins as indicated, before and after microinjection of WCA/Rac1. Time equals minutes and seconds, and bars in each case correspond to 10 μm .

Movie S7: Phase contrast movies of fish keratocytes injected with Rac1 or WCA/Rac1, as indicated. Time is in minutes and seconds, bar: 10 μm .

Figure S1

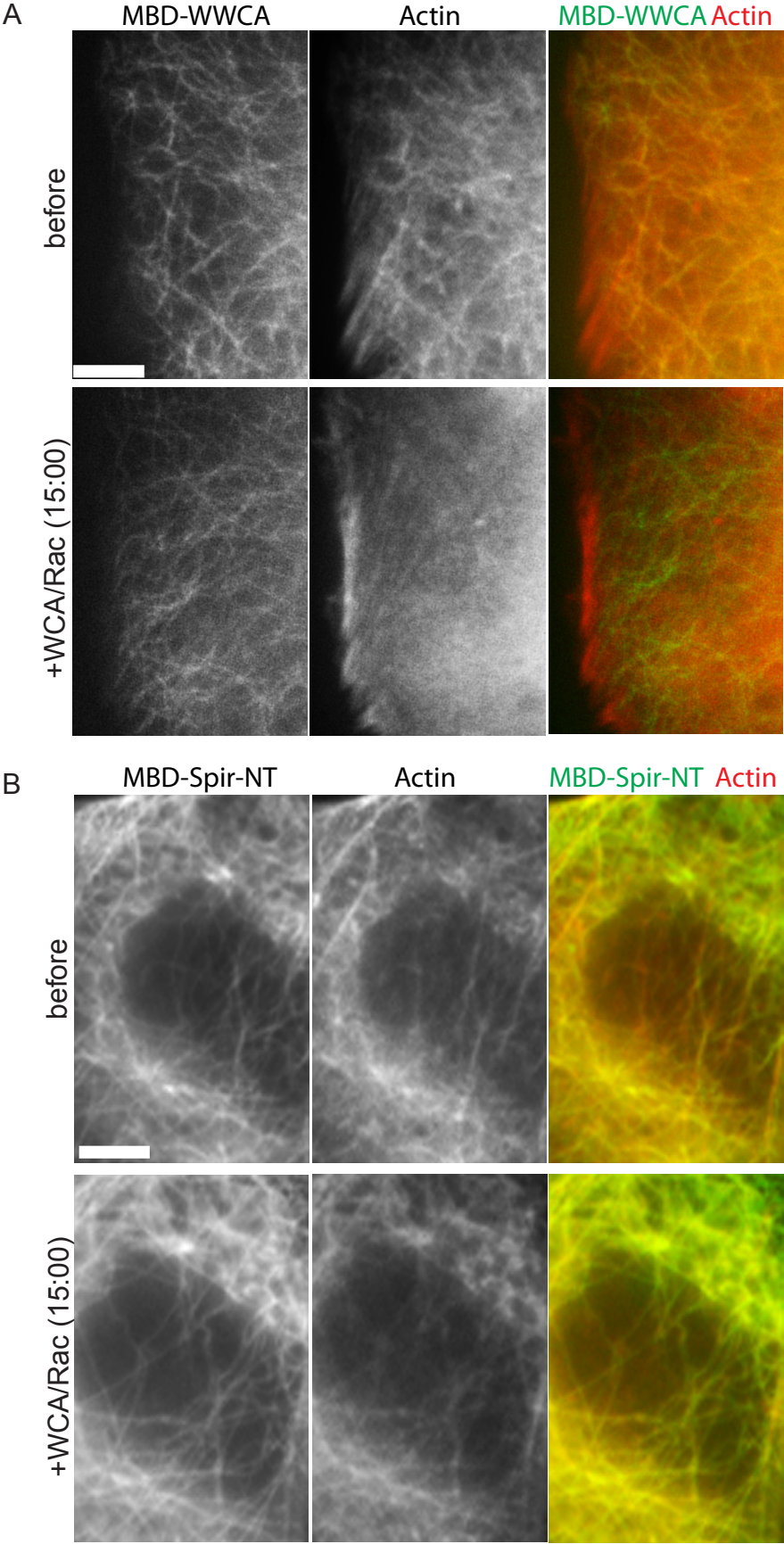


Figure S2

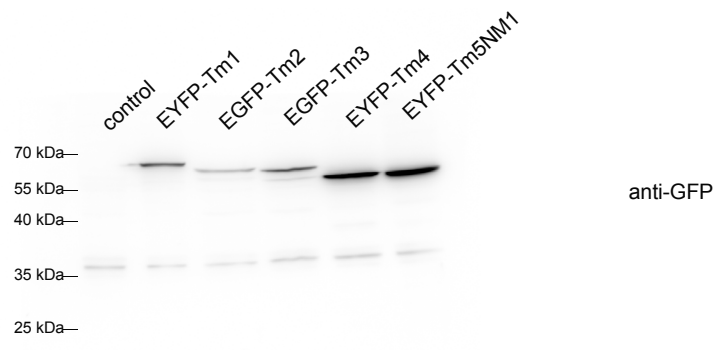
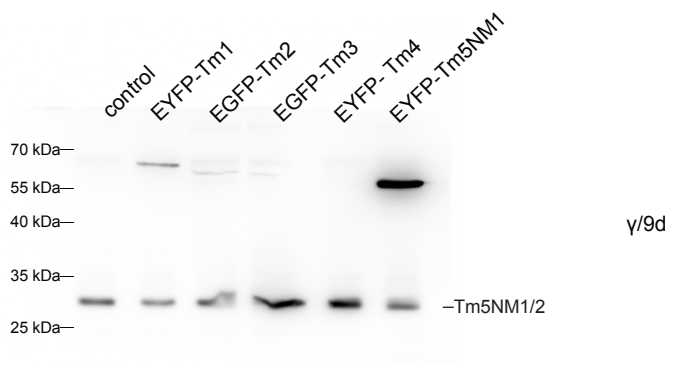
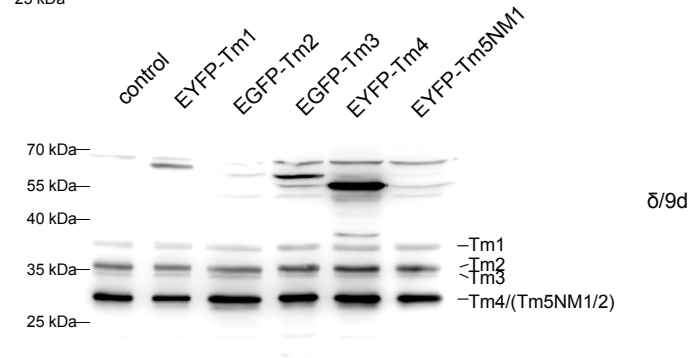
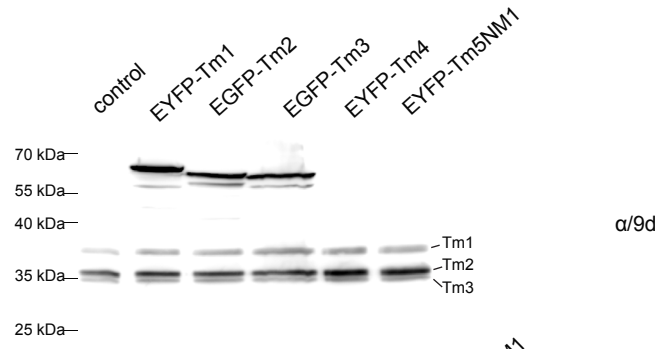


Figure S3

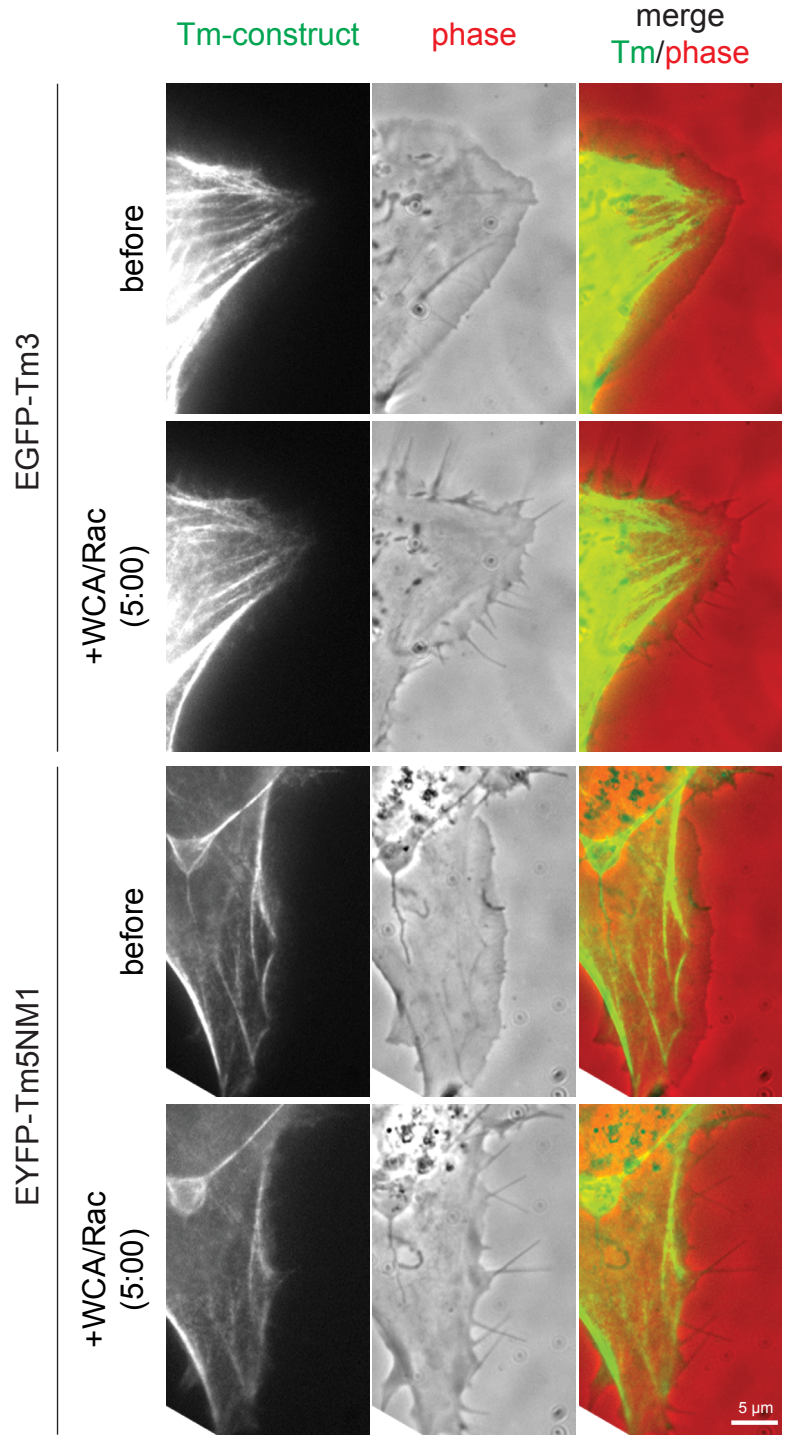


Figure S4

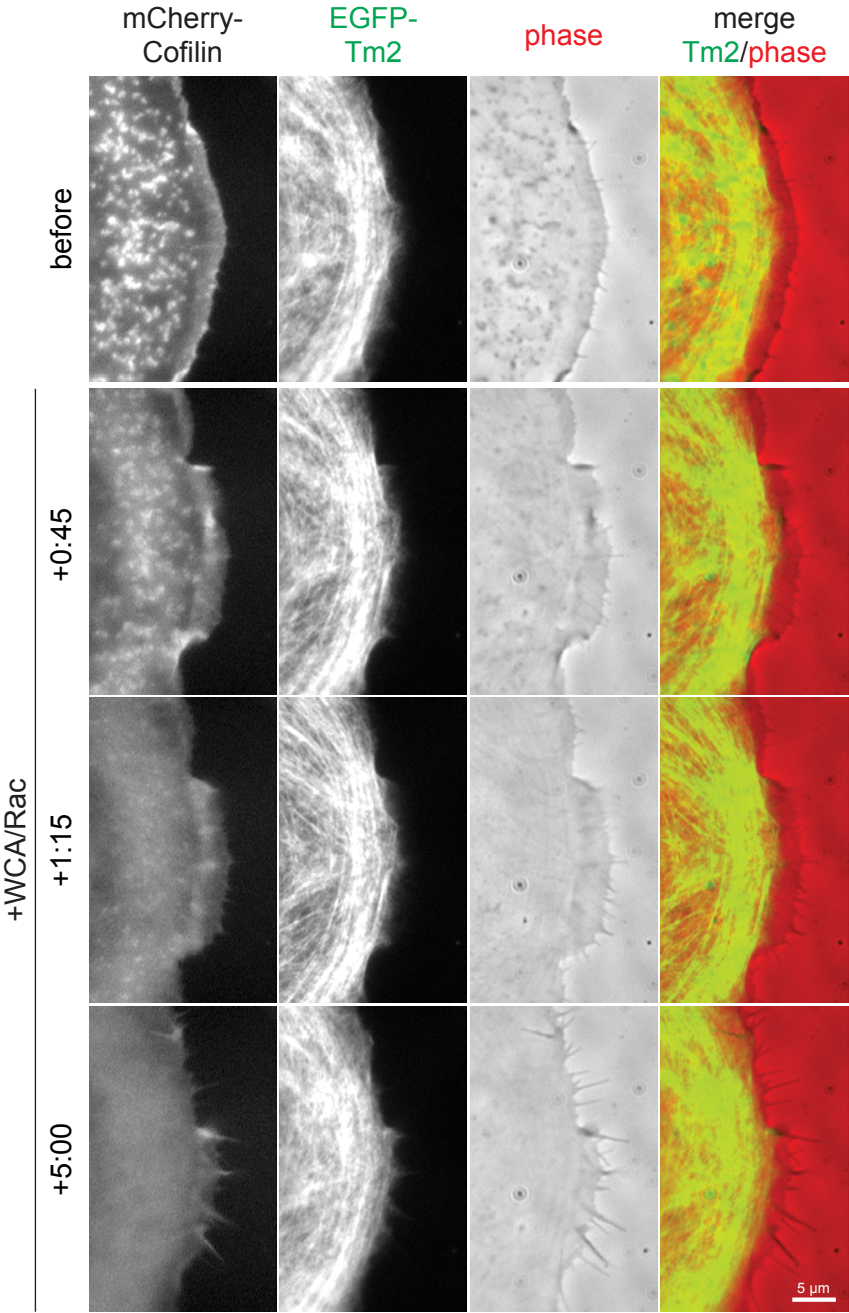


Figure S5

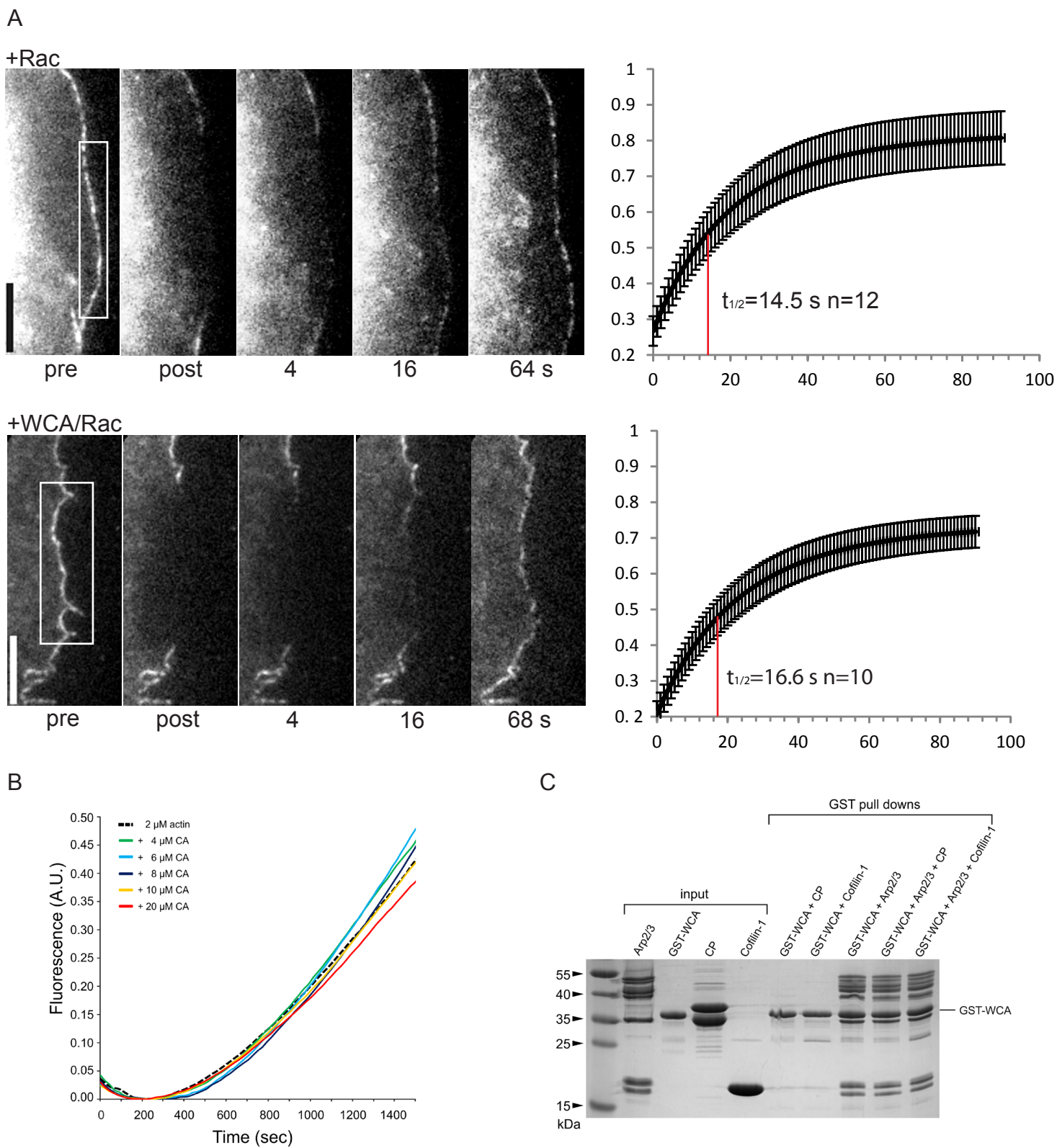


Figure S6

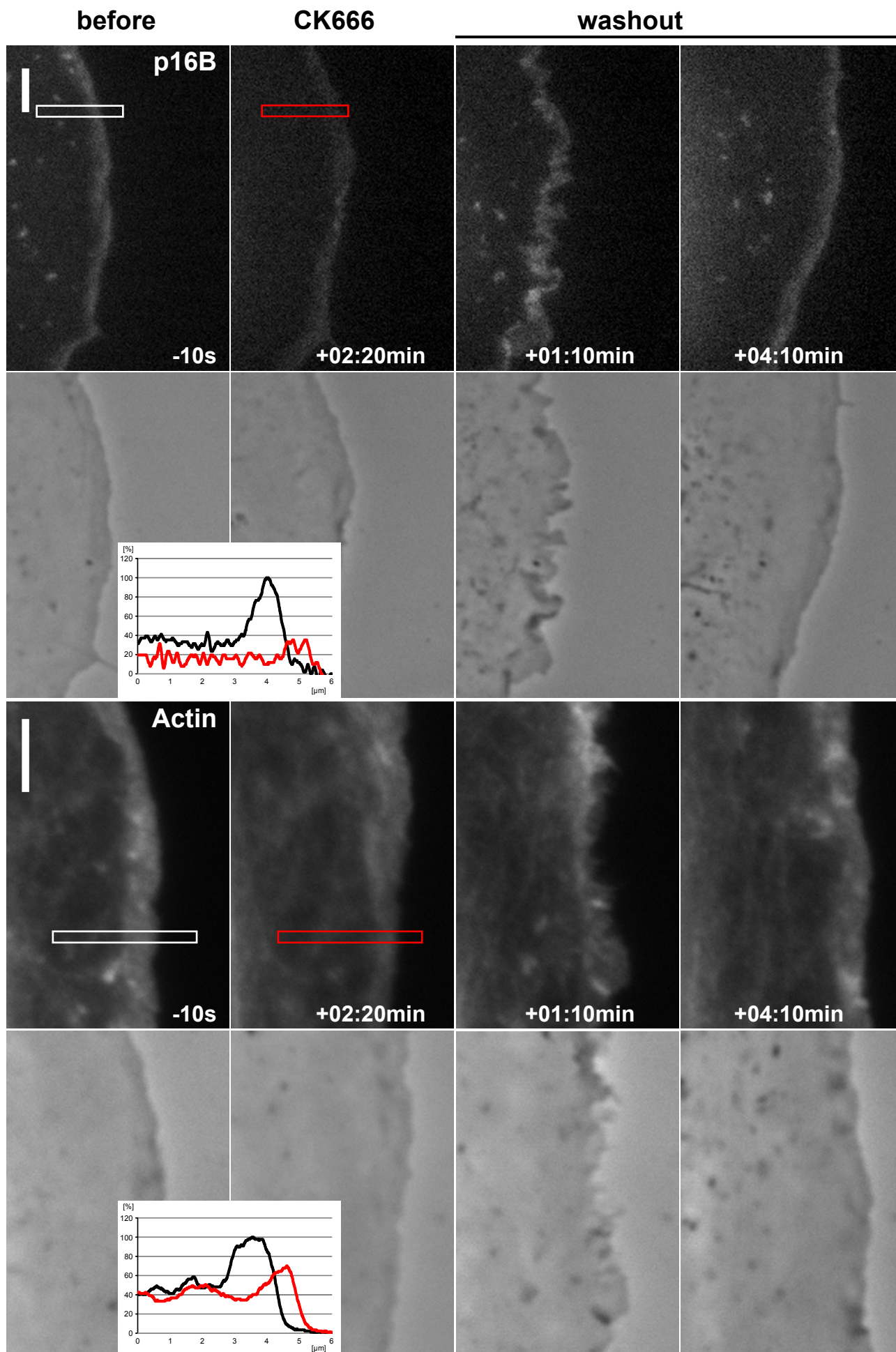


Figure S7

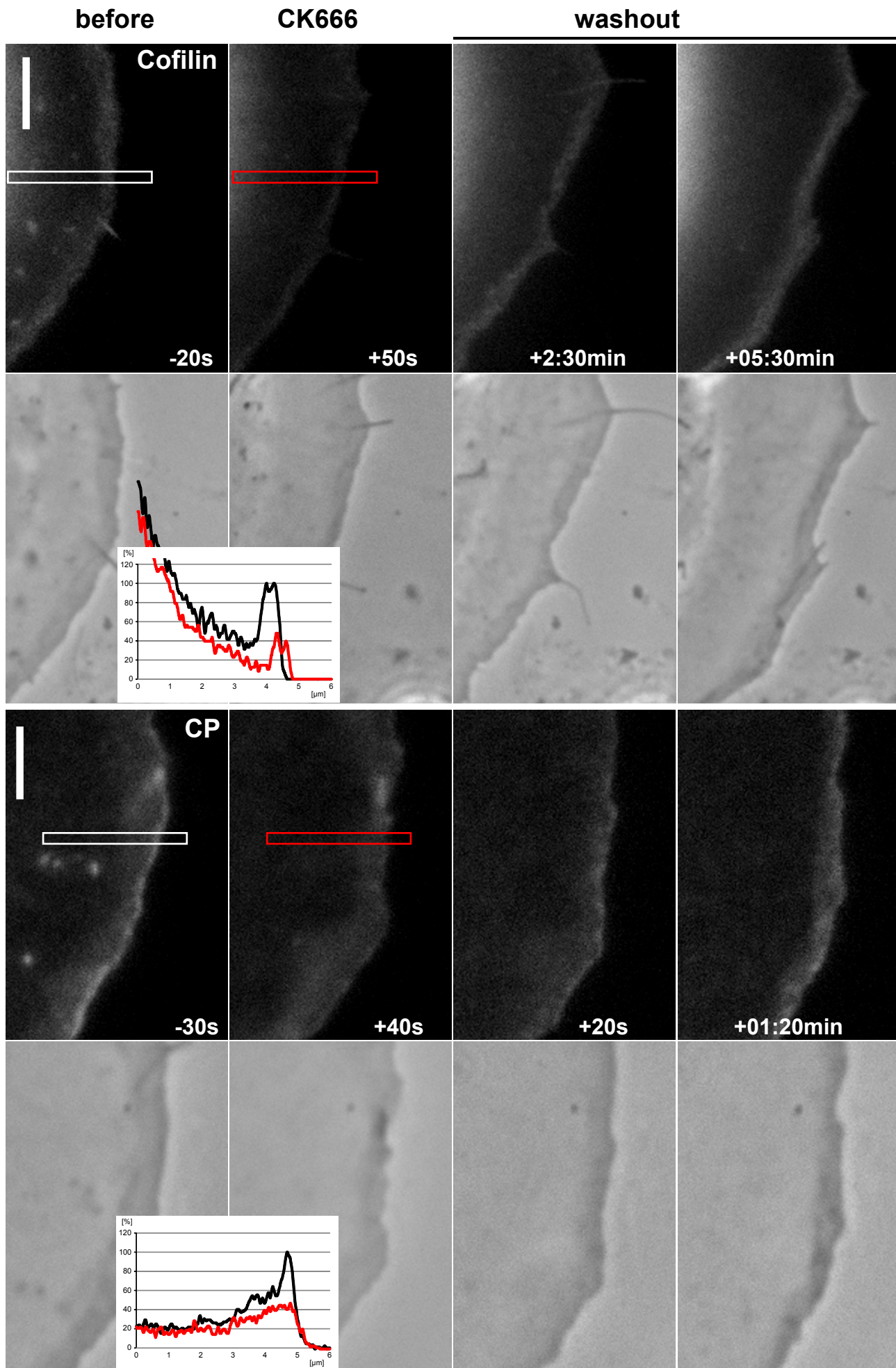
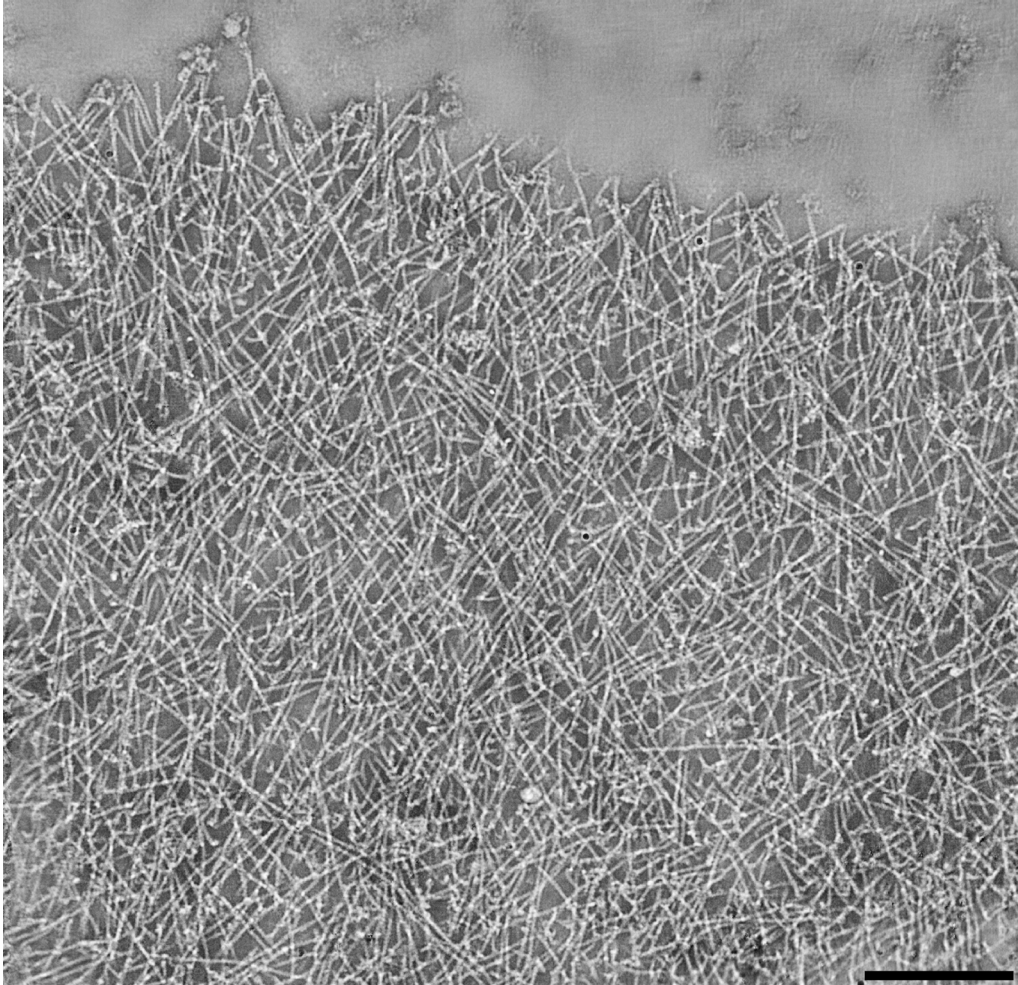
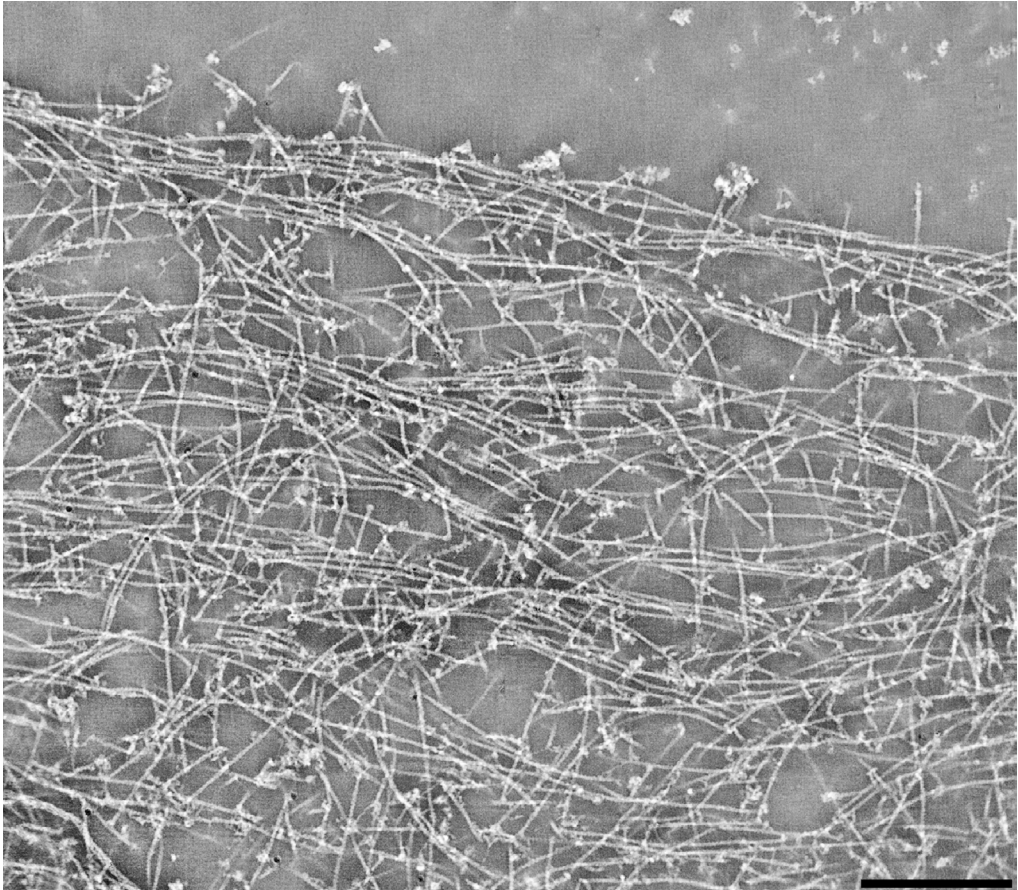


Figure S8



+Rac



+WCA/Rac